Rapid Publication

Independent Development of Pancreatic α- and β-Cells From Neurogenin3-Expressing Precursors

A Role for the Notch Pathway in Repression of Premature Differentiation

Jan Jensen, R. Scott Heller, Tove Funder-Nielsen, Erna E. Pedersen, Claire Lindsell, Gerry Weinmaster, Ole D. Madsen, and Palle Serup

The nature and identity of the pancreatic β-cell precursor has remained elusive for many years. One model envisions an early multihormonal precursor that gives rise to both α- and β-cells and the other endocrine cell types. Alternatively, β-cells have been suggested to arise late, directly from the GLUT2- and pancreatic duodenal homeobox factor-1 (PDX1)-expressing epithelium, which gives rise also to the acinar cells during this stage. In this study, we have identified a subset of the PDX1$^+$ epithelial cells that are marked by expression of *Neurogenin3* (*Ngn3*). *Ngn3*, a member of the basic helix-loop-helix (bHLH) family of transcription factors, is suggested to act upstream of *NeuroD* in a bHLH cascade. Detailed analysis of *Ngn3*/paired box factor 6 (PAX6) and *NeuroD*/PAX6 co-expression shows that the two bHLH factors are expressed in a largely nonoverlapping set of cells, but such analysis also suggests that the *NeuroD*$^+$ cells arise from cells expressing *Ngn3* transiently. *NeuroD*$^+$ cells do not express Ki-67, a marker of proliferating cells, which shows that these cells are postmitotic. In contrast, Ki-67 is readily detected in *Ngn3*$^+$ cells. Thus, *Ngn3*$^+$ cells fulfill the criteria for an endocrine precursor cell. These expression patterns support the notion that both α- and β-cells develop independently from PDX1$^+$/*Ngn3*$^+$ epithelial cells, rather than from GLU$^+$/INS$^+$ intermediate stages. The earliest sign of α-cell development appears to be Brain4 expression, which apparently precedes Islet-1 (ISL1) expression. Based on our expression analysis, we propose a temporal sequence of gene activation and inactivation for developing α- and β-cells beginning with activation of *NeuroD* expression. Endocrine cells leave the cell cycle before *NeuroD* activation, but re-enter the cell cycle at perinatal stages. Dynamic expression of *Notch1* in PDX$^+$ epithelial cells suggests that Notch signaling could inhibit a Ngn-NeuroD cascade as seen in the nervous system and thus prevent premature differentiation of endocrine cells. *Diabetes* 49:163–176, 2000

Morphologically, the cells of the developing rodent pancreas have been described to pass through two transitions at separate time points (1,2). Between the 6- and 10-somite stages, cells at the proper regions of the posterior foregut become restricted to the pancreatic lineage (3). Subsequently, an evagination of the epithelium at the 22- to 25-somite stage generates the cells of the "proto-differentiated" epithelium. At this stage (the primary transition), the first glucagon-producing endocrine cells also appear. The proto-differentiated epithelium grows and branches until the secondary transition (4), which occurs between embryonic day (E) 13.5 and E15.5 in the mouse. At this time, cell types characterized by mature secretory granules are generated.

Based on immunohistochemical analysis of hormone expression in the developing pancreas (5,6) and the multihormonal phenotype of most pancreatic endocrine tumors (7,8), we and others have previously suggested that the β-cell originates from early multihormonal precursor cells. It was thought that all of the islet endocrine cells would be related in a direct lineage relationship. However, more recent studies in transgenic mice that used the glucagon (GLU) or insulin (INS) promoter to drive expression of the diphtheria-toxin A-chain contradict this model. The respective lack of either α- or β-cells in these mice suggests that α- and β-cells derive independently (9). Moreover, early appearing GLU$^+$ cells do not divide, which makes it difficult to envision a significant contribution from these to the vast increase in β-cell mass seen during the secondary transition (10). More

From the Department of Developmental Biology (J.J., R.S.H., T.F.-N., E.E.P., O.D.M., P.S.), Hagedorn Research Institute, Gentofte, Denmark; and the Department of Biological Chemistry (C.L., G.W.), University of California at Los Angeles School of Medicine, Los Angeles, California.

Address correspondence and reprint requests to Dr. Palle Serup, Hagedorn Research Institute, Niels Steensensvej 6, DK-2820 Gentofte, Denmark. E-mail: pas@hagedorn.dk.

Received for publication 1 November 1999 and accepted in revised form 24 November 1999. Posted on the World Wide Web at www.diabetes.org/diabetes on <<date.>

J.J., R.S.H., T.F.-N., E.E.P., O.D.M., and P.S. are employed by Hagedorn Research Institute, an independent research component of Novo Nordisk A/S, Denmark.

bHLH, helix-loop-helix; BrdU, 5-bromo-2′-deoxyuridine; *Brn4* , *Brain4/Pou3f4* ; DEPC, diethyl pyrocarbonate; E, embryonic day; GLU, glucagon; INS, insulin; ISL1, Islet-1; *Ngn3* , *Neurogenin3* ; PAX6, paired box factor 6; PBS, phosphate-buffered saline; PDX1, pancreatic duodenal homeobox factor-1; PFA, paraformaldehyde; RT-PCR, reverse transcriptase–polymerase chain reaction; SSC, sodium chloride–sodium citrate.

recent immunohistochemical analyses have suggested that β-cells arise directly from the proto-differentiated epithelial cells, which express the β-cell markers GLUT2, TrkA , PDX1, and Nkx6.1 (11–15). However, because these cells also give rise to the acinar cells, the signals that determine the endocrine fate remains unknown. Lately, studies of pancreas development in mice deficient for *Isl1* have hinted at a transcription factor cascade that operates in endocrine differentiation. *Isl1* $^{-/-}$ mice (10) lack *Pax6* expression but retain *NeuroD* expression (16), which suggests that *NeuroD* acts upstream and *Pax6* acts downstream of *Isl1* . Furthermore, clues to factors acting upstream of *NeuroD* have come from studies of neural development. The Neurogenin family of bHLH factors is thus required for expression of NeuroD family factors in certain neuronal subtypes (17,18).

In this study, we found that the bHLH gene *Neurogenin3/MATH4B/Atoh5* (*Ngn3*) is expressed in a subset of the proto-differentiated PDX1$^+$ epithelial cells. Ki-67, a marker of proliferating cells, is readily detected in *Ngn3*$^+$ cells but not in *NeuroD*$^+$ cells. A few *Ngn3*$^+$ cells co-express early endocrine markers, such as ISL1 and PAX6, whereas no *Ngn3*$^+$ cells co-express GLU or INS. In contrast, we found that *NeuroD* is co-expressed with PAX6 and glucagon or insulin. However, a few *NeuroD*$^+$ cells do not express PAX6, which suggests that *NeuroD* is the earliest marker of differentiating endocrine cells. Furthermore, we found evidence for a temporal sequence of gene activation and inactivation that differs between α- and β-cells. Together, these findings suggest a molecular pathway where *Ngn3*$^+$ precursor cells become committed to endocrine differentiation marked by activation of *NeuroD* and subsequently *Isl1* , *Pax6* , and the hormones, whereas *Ngn3* expression is extinguished. The choice between α- and β-cell fate likely depends on a transcription factor code where *Brain4/Pou3f4* (*Brn4*) determines α-cell development and *Pdx1* , *Nkx6.1* , and *Pax4* determine β-cell development. Expression of *Notch1* in the epithelial cells suggests that the choice between differentiation and continued proliferation could be controlled by a Jagged-Notch-HES1 pathway that inhibits Ngn3 function.

RESEARCH DESIGN AND METHODS

Animals and pancreas microdissection. Time-mated pregnant mice (CD1) and rats (Wistar-Furth) were obtained from Bomholtgård Breeding Centre (Ry, Denmark). Embryos (one litter at a time) were liberated in chilled Hanks' balanced salt solution; pancreases were collected by microdissection and were transferred directly to RNAzol-B (Biotecx, Houston, TX) for reverse transcriptase–polymerase chain reaction (RT-PCR) analyses. Material used for histological analysis was fixed overnight in 4% paraformaldehyde (PFA) before paraffin-embedding. Sections of 4 µm were cut and stored at room temperature until use. Material for whole-mount in situ hybridizations was fixed overnight in 4% PFA in Ca^{2+} and Mg^{2+} free phosphate-buffered saline (PBS) and 2 mmol/l EGTA. The tissues were dehydrated in methanol and stored at –20°C until use. For RT-PCR, rat pancreatic tissue originating from the dorsal bud was isolated before fusion; at later stages, tissue from the prominent splenic portion, which was also dorsally derived, was used. At the earliest time points (E12.5 and E13.5), a full litter (~10–12) of isolated pancreatic buds was combined due to the small amount of tissue. At later stages, fewer pancreases were used, and after E17.5, isolations were performed on material from a single organ. No separation of the pancreatic mesenchyme was performed. However, at later stages, the portion of the mesenchyme that was condensed to form the spleen and that was visible during E14–16 was removed. At least two independent cDNA preparations from the different time points were analyzed (except at E12.5).

Antisera and in situ hybridization probes. Guinea pig anti-insulin was obtained from Nordisk Gentofte A/S (Gentofte, Denmark). Mouse monoclonal antiglucagon-Glu001 was obtained from Novo Nordisk A/S (Bagsværd, Denmark). Rabbit anti-PDX1-1856 and rabbit anti-Nkx6.1-174 have been described previously (19). Rabbit anti-IDX1-253 (20) was a kind gift from J. Habener. Rabbit anti-BRN4 was a kind gift from M. Rosenfeld. Rabbit anti-PAX6-Bg11 (21) was a kind gift from S. Saule. Rabbit anti-ISL1 (22) was a kind gift from H. Edlund. Mouse monoclonal anti-ISL1, developed by T. Jessell, was obtained from the Developmental Studies Hybridoma Bank, which is under the auspices of the National Institute of Child Health and Human Development and maintained by the Department of Biological Sciences at the University of Iowa (Iowa City, IA). Mouse monoclonal anti–5-bromo-2′-deoxyuridine (BrdU)-Bu20A was from DAKO A/S (Glostrup, Denmark). Mouse monoclonal anti-Ki-67-B56 was from Pharmingen (San Diego, CA).

Plasmids for synthesis of digoxigenin-labeled riboprobes, such as mouse Ngn3, rat NeuroD, and rat Notch-1 and -2, were kindly donated by F. Guillemot, F.G. Andersen, and J. Hald, respectively. The Ngn3 plasmid was cut with *Hind* III and transcribed with SP6 RNA polymerase; the NeuroD plasmid was cut with *Bam* HI and transcribed with T7 RNA polymerase; the Notch-1 and -2 plasmids were cut with *Bam* HI and *Spe* I, respectively, and transcribed with T7 RNA polymerase in the presence of digoxigenin-UTP (Boehringer Mannheim, Mannheim, Germany).

Immunohistochemistry and in situ hybridization. Essentially, immunohistochemistry was performed as previously described (23). Briefly, sections were dewaxed in xylene and rehydrated through a descending ethanol series. Antigen retrieval was accomplished through microwave treatment (two times for 5 min at 600 W in 0.01 mol/l citrate buffer, pH 6.0) followed by three washes in PBS. Nonspecific binding was blocked with 10% donkey nonimmuneserum. For double immunofluorescence, sections were incubated with primary antibodies overnight. Secondary antibodies (fluorescein isothiocyanate–, Cy-2-, and Texas-Red-conjugated) were obtained from Jackson ImmunoResearch (West Grove, PA). In situ hybridization on paraffin sections was performed by first dewaxing and rehydrating paraffin sections through an ethanol series. Three washes in diethyl pyrocarbonate (DEPC)-treated PBS were followed by a 5–10 min treatment with proteinase K (10 µg/ml). Slides were fixed in fresh 4% paraformaldehyde and rinsed in DEPC PBS. Sections were acetylated for 10 min and permeabilized with Triton X 100 (1%) for 30 min. Prehybridization was for 2 h, and slides were incubated with digoxigenin-labeled antisense riboprobes overnight at 72°C in a humidified chamber. The unhybridized probe was removed with subsequent rinses in 5× sodium chloride–sodium citrate (SSC) and 0.2× SSC at 72°C for 1 h each. Slides were rinsed in Tris-buffered saline with Tween with 2 mmol/l Levimasole (Sigma, St. Louis, MO) and blocked with 10% heat-inactivated sheep serum. Alkaline phophatase–conjugated Fab fragments (Boehringer Mannheim), preabsorbed with E17 embryo powder, were added to the slides overnight at 4°C. Slides were rinsed in NTMT (0.1 mol/l NaCl, 0.02 mol/l Tris [pH 9.5], 0.01 mol/l $MgCl_2$, and 1% Tween-20) three times for 10 min, and the reaction mixture was added (nitroblue tetrazolium and 5-bromo-4-chloro-3-indolylphosphate [Boehringer Mannheim] in NTMT). Reactions were allowed to proceed for 2 h to 5 days at room temperature. The reaction was stopped by several rinses in Tris-EDTA, and slides were mounted and coverslipped. Whole-mount in situ hybridizations on mouse embryos were performed as previously described (24). Subsequently, the whole-mount specimens were cryo-protected in 30% sucrose in 0.1 mol/l phosphate buffer overnight and embedded in Tissue-Tek (Sakura Finetek Europe, Zoeterwoude, the Netherlands), and 10-µm sections were cut on a cryostat. Sections were frozen and stored at –80°C. Images were collected by using an Olympus BX60 microscope (Olympus Optical, Tokyo) equipped with a Hamamatsu-chilled C5810 Color CCD camera (Hamamatsu Photonics, Solna, Sweden), and images were processed using the IMAGE-Pro PC software package (Media Cybernetics, Silver Spring, MD) and Adobe Photoshop 3.0 (Adobe Systems, San Jose, CA). False color images were generated in Adobe Photoshop 3.0 by using the invert and selective color algorithms.

RNA isolation and cDNA synthesis. RNA was isolated from the microdissected embryonic tissue using the RNAzolB single-step method (Biotecx). Tissue was transferred to chilled eppendorfs containing 100 µl RNAzol-B and were homogenized using motor-driven micropistils (Eppendorf, Hamburg, Germany). Chloroform (10 µl) was added, followed by vortexing and 5′ centrifugation at 10,000 rpm. The aqueous phase was precipitated using 1 volume isopropanol, and subsequently reprecipitated by 2.5 volumes of ethanol and 0.1 volume of 4 mol/l NaCl. Total RNA pellets were dissolved using DEPC-treated water. cDNA synthesis was performed on 1 µg total RNA as described in a previous study (19).

Multiplex RT-PCR. Multiplex RT-PCR was performed as described by Jensen et al. (19), though with a few changes in the described procedure. The reaction volume was lowered to 25 µl. All final concentrations of buffers, dNTPs, and primers were unchanged. The template concentration was decreased accordingly (the template per reaction was 1/50th of the cDNA reaction performed on 1 µg total RNA). All reactions were performed in 0.2-ml microtube strips (Stratagene) or 96-well plates, and mineral oil was included during cycling. The thermal-cycling profile was set at 1′ denaturation at 96°C, followed by the selected number of cycles: 30 s at 96°C, 30 s at 55°C, and 30 s at 72°C. The increase in denaturing temperature has shown an improved amplification of G/C rich amplicons. All pipet-

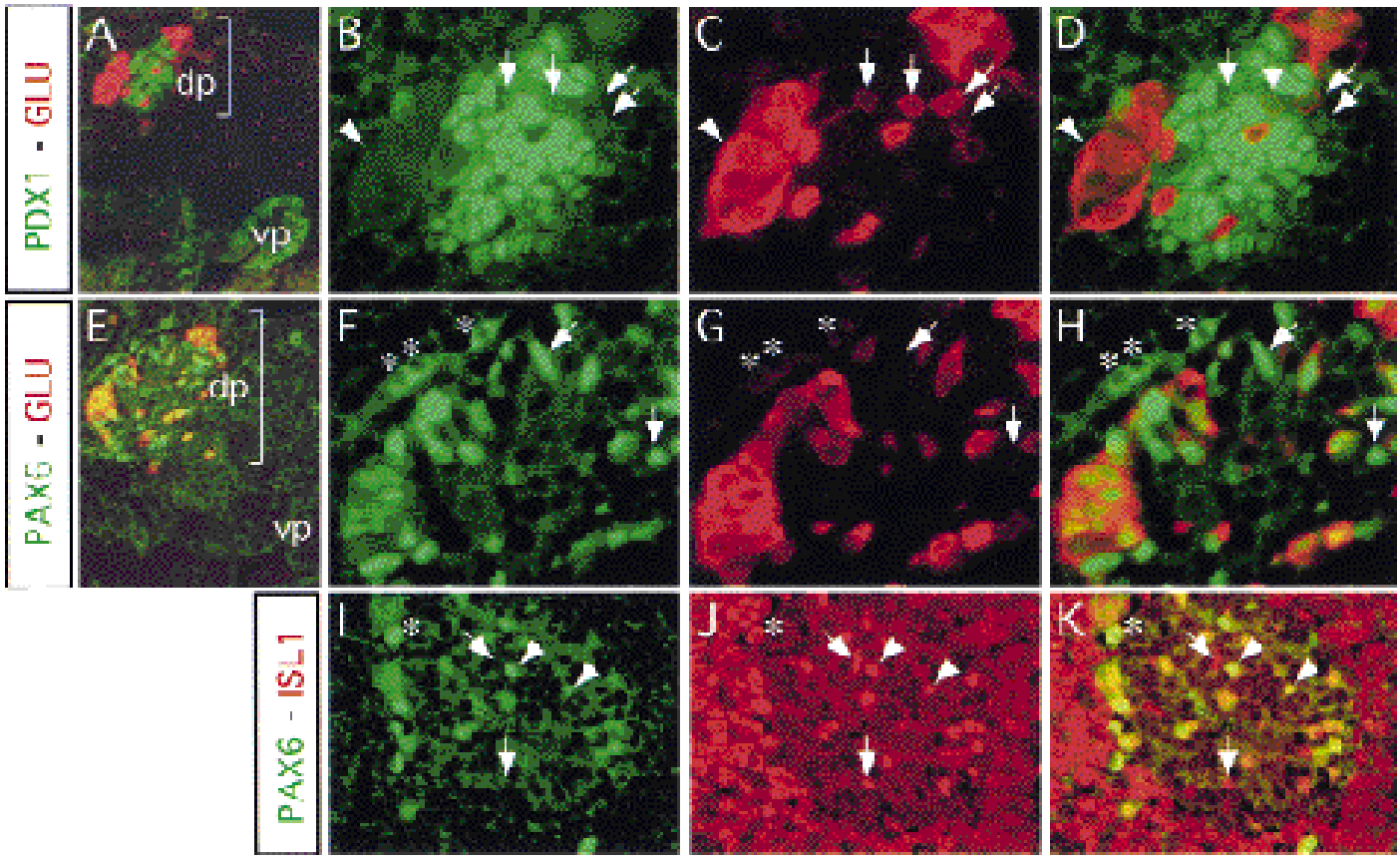

FIG. 1. Expression of PDX1, PAX6, ISL1, and glucagon in E10 mouse pancreas. *A*: Transverse section stained for PDX1 (green) and glucagon (red) illustrates that glucagon-expressing cells are restricted to the dorsal pancreas (dp), whereas PDX1 is expressed in both the dorsal and ventral pancreas (vp). The bracket indicates the dorsal region shown in higher magnification (*B–D*). *B–D*: Higher magnification of the bracketed region in *A*. Some GLU$^+$ cells express low amounts of PDX1 (arrows), whereas most GLU$^+$ cells are PDX1$^-$ (arrowhead). *E*: Transverse section stained for PAX6 (green) and glucagon (red) illustrates that PAX6-expressing cells are restricted to the dorsal pancreas (dp). The bracket indicates the dorsal region shown in higher magnification (*F–H*). *F–H*: Higher magnification of the bracketed region in *E*. All GLU$^+$ cells express PAX6, whereas some PAX6$^+$ cells are GLU1$^-$ (arrows). *I–K*: Section stained for PAX6 and ISL1 illustrates that all PAX6$^+$ cells express ISL1 (arrowheads), whereas some ISL1$^+$ cells are PAX6$^-$ (arrows). *Red blood cells.

ting steps in the RT-PCR analyses were performed using a multichannel pipette. To increase accuracy, no pipetting volumes were set below 3 µl. Sequencing gel runs were performed as described by Jensen et al. (19). For neurogenin-3, 160 bp, the primer sequence (upstream primer listed first) was 5′-TGGCGCCTCATCCC TTGGATG-3′, 5′-CAGTCACCCACTTCTGCTTCG (Genbank no. U76208); for HES-1, 270 bp, the primer sequence was 5′-TCAACACGACACCGGACAAACC-3′, 5′-GGTACTTCCCCAACACGCTCG-3′ (Genbank no. D13417); for p48/PTF-1, 249 bp, the primer sequence was 5′-AAGGTCATCATCTGCCATCGAG-3′, 5′-AGCCG GCCTGTGAGAGCTTTC-3′ (Genbank no. X98446); for MASH-1, 220 bp, the primer sequence was 5′-GTCGAATACATCCGCGCGCTG-3′, 5′-AGAACCAGTTG GTAAAGTCCA-3′ (Genbank no. X53725); for amylase, 300 bp, the primer sequence was 5′-GAGGACATGGTGCTGGAGGAG-3′, 5′-CGTTGACTACATTCCT GAAGG-3′ (Genbank no. M24962); for c-Met, 230 bp, the primer sequence was 5′-TTATGGACCCAACCACGAGCAC-3′, 5′-GAAGCGACCTTCTGATGTCCC-3′ (Genbank no. S69881); for Isl-2, 272 bp, the primer sequence was 5′-GCAGCCA GTATCTGGATGAGAC-3′, 5′-CTCCAGCAGGAGGCCGTGGT-3′ (Genbank no. L35571); for Notch-1, 170 bp, the primer sequence was 5′-CTGGTTCCCTGAGG GTTTCAA-3′, 5′-GGAACTTCTTGGTCTCCAGGT-3′ (Genbank no. X57405); for Notch-2, 190 bp, the primer sequence was 5′-CAACATGGGCCGCTGTCCTC-3′, 5′-CACATCTGCTTGGCAGTTGATC-3′ (Genbank no. M93661); for Notch-3, 230 bp, the primer sequence was 5′-GCAGCTGTGAACAACGTGGAG-3′, 5′-AACCGCAC AATGTCCTGGTGC-3′ (Genbank no. X74760); and for Jagged-1, 270 bp, the primer sequence was 5′-AAGCCACGTGTAATAACGGTGG-3′, 5′-CTCCATCCAC ACAGGTTCCGC-3′ (Genbank no. L38483).

Primer sequences for INS, GLU, NeuroD, G6PDH, tubulin, Sp-1, TBP, and Id-1, -2, -3, and -4 are described in the study by Jensen et al. (19). Primer sequences for ngn, ngn-2, NeuroD2/NDRF, MATH-1, MASH-2, HES-2, HES-3, HES-5, and Notch-4 are available upon request from jnj@hagedorn.dk.

RESULTS

The earliest glucagon-expressing endocrine cells arise with a scattered distribution from PDX1-expressing epithelial cells. Using double immunofluorescence staining for glucagon and insulin together with the nuclear markers PDX1, ISL1, PAX6, and BRN4, we analyzed the development of the earliest endocrine cells in the mouse pancreas at the budding stage. As seen in Fig. 1*A*, both the dorsal and ventral pancreatic bud are clearly defined at E10 by PDX1 immunoreactivity. The dorsal bud is larger, contains more PDX1$^+$ cells, and is more mature than the ventral bud because GLU$^+$ cells are found in only the dorsal bud (Fig. 1*A*). Most glucagon cells are devoid of PDX1, but some PDX1$^+$/GLU$^+$ cells are found (Fig. 1*B–D*), suggesting that the GLU$^+$ cells derive from the PDX1$^+$ cells and subsequently lose PDX1 expression. The GLU$^+$ cells at this stage are mitotically quiescent, as determined by the lack of BrdU incorporation (10), and none express insulin at significant levels (data not shown). Evidence for a temporal sequence of gene activation comes from GLU/PAX6 and PAX6/ISL1 double immunofluorescent stainings. GLU$^+$ cells invariably express ISL1 (data not shown) (10) and PAX6 (Fig. 1*E–H*). However, the presence of GLU$^-$/PAX6$^+$ (Fig. 1*E–H*) and PAX6$^-$/ISL1$^+$

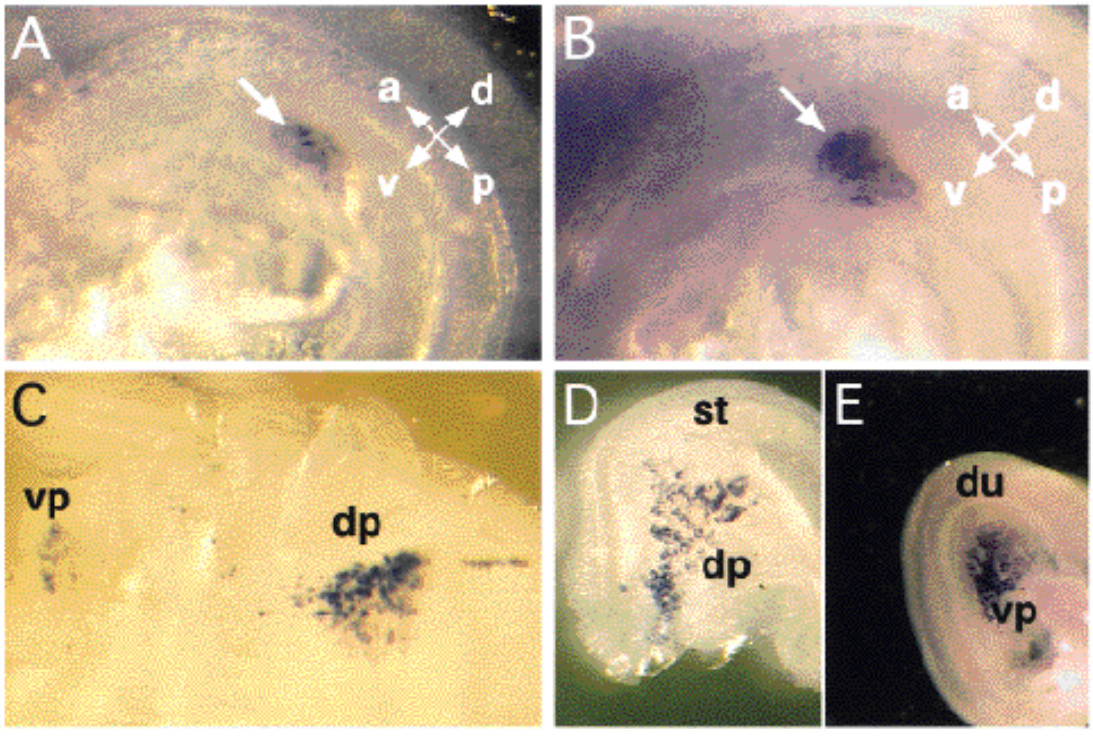

FIG. 2. *Neurogenin3* expression in mouse embryonic pancreas between E9.5 and E15.5 as detected by whole-mount in situ hybridization. *A*: Expression is first detected in the dorsal pancreatic bud at E9.5 (arrow). *B*: At E10.0, expression in the dorsal bud has increased in size (arrow) and *Ngn3* expression has intensified. Dorsal, ventral, anterior, and posterior directions are indicated in *A* and *B*. *C*: At E13.5, *Ngn3* expression is evident in both the dorsal (dp) and ventral (vp) pancreas. *D* and *E*: Dorsal (*D*) and ventral (*E*) pancreas at E15.5 express high levels of *Ngn3* mRNA. st, Stomach; du, duodenum.

(Fig. 1*I–K*) cells suggests that ISL1 expression precedes PAX6, which, as previously mentioned, precedes glucagon production.

Neurogenin3 is a marker of endocrine precursor cells. The involvement of bHLH transcription factors in the development of endocrine cells is well established (25–30). In contrast to PAX6, *NeuroD* expression is present in *Isl1* $^{-/-}$ mice (16), which suggests that bHLH factors act upstream of *Isl1* . We performed an RT-PCR screening for atonal-like bHLH factors in various stages of embryonic pancreas and found that *Ngn3* and *NeuroD* were strongly expressed (data not shown), which is in agreement with previously published results (28–31). The spatial pattern of *Ngn3* and *NeuroD* expression was determined by whole-mount in situ hybridization. At the earliest stage examined (E9.5), we found *Ngn3* expressed in a speckled pattern in the dorsal pancreatic bud exclusively (Fig. 2*A*). A similar profile, though with increased expression, was observed at E10.0 (Fig. 2*B*). At E13.5 (Fig. 2*C*) and E15.5 (Fig. 2*D* and *E*), expression was evident in both the dorsal and ventral pancreas. Through stages E9.5–E15.5, we observed an increase in the expression level of *Ngn3* . RT-PCR analysis confirmed the increase in *Ngn3* expression until E15 (data not shown). At E17, only a small part of the epithelium showed detectable *Ngn3* expression and at a low intensity (data not shown). Pancreatic expression of *NeuroD* examined by whole-mount in situ hybridization was superficially similar to the *Ngn3* expression (data not shown). To determine the cellular localization of *Ngn3* and *NeuroD* expression, we sectioned the whole-mount in situ hybridized embryos and performed immunohistochemical stainings with antisera against PDX1, PAX6, and glucagon.

At E10.0, the *Ngn3* $^{+}$ cells were found in clusters and co-localized with a subset of the PDX1^{+} cells (Fig. 3*A–D*). In contrast, *Ngn3* expression in PAX6^{+} and GLU^{+} cells was low or absent (Fig. 3*E–L*). At E13.5, PAX6^{+} cells were mostly outside the *Ngn3* $^{+}$ domain (Fig. 4*A–D*). However, a few PAX6^{+} cells were clearly coexpressing *Ngn3* (Fig. 4*A–D*), which suggests that endocrine cells derive from the *Ngn3* $^{+}$ cells and subsequently lose *Ngn3* expression. In contrast, PAX6^{+} cells (GLU^{+} and GLU^{-}) also express *NeuroD* (Fig. 4*E–H*). Occasionally, we found *NeuroD* $^{+}$ cells that did not express PAX6 (Fig. 4*E–H*), which supports the notion that *NeuroD* acts upstream of ISL1 and PAX6. A similar profile was observed at the peak of *Ngn3* expression (E15.5), when PAX6^{+} cells (with a few exceptions) were outside the *Ngn3* $^{+}$ domain (Fig. 4*I–L*) and GLU^{+} and INS^{+} cells are excluded from the *Ngn3* $^{+}$ domain (Fig. 4*M–P*). At E17.5, when *Ngn3* expression was found only in a small part of the epithelium, we again found that PAX6^{+} and INS^{+} cells are excluded from the *Ngn3* $^{+}$ domain (Fig. 5*A–D*), but they overlap with the *NeuroD* $^{+}$ domain (Fig. 5*E–H*). GLU^{+} cells also were excluded from the *Ngn3* $^{+}$ domain at this stage, whereas Nkx6.1^{low} cells can be found in some but not all *Ngn3* $^{+}$ cells (Fig. 5*I–L*). In contrast, Nkx6.1^{high} cells are always outside the *Ngn3* $^{+}$ domain (Fig. 5*I–L*), but inside the *NeuroD* $^{+}$ domain (Fig. 5*M–P*). At all stages examined, we found endocrine cells located at close proximity to the *Ngn3* $^{+}$ cells, which is consistent with a role for the *Ngn3* $^{+}$ cells as precursors for the endocrine cells. *Ngn3* expression was never observed in the pancreatic acinar cells at E15.5 or later.

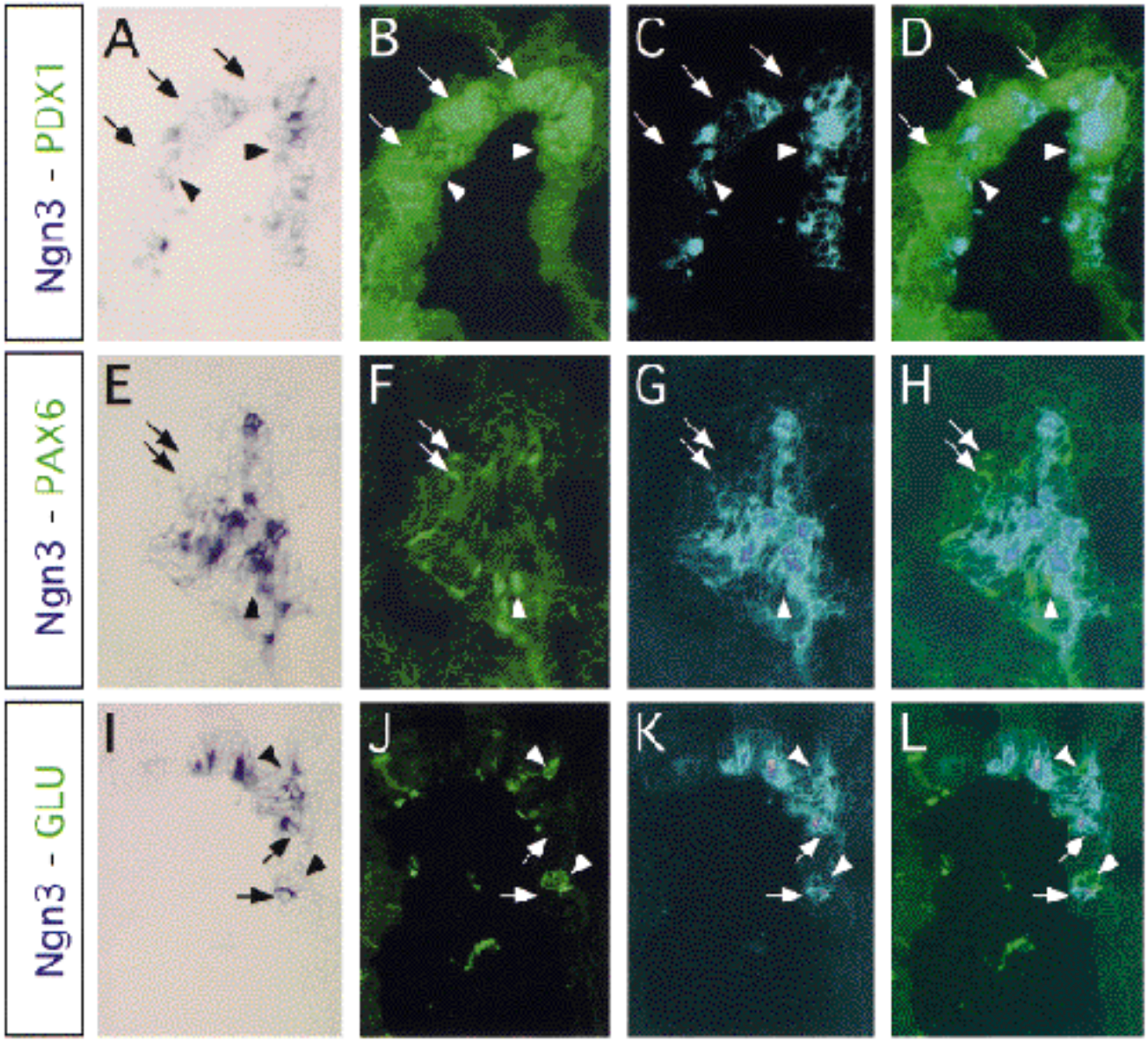

FIG. 3. *Neurogenin3* expression in E10.0 dorsal pancreas as detected in sections after whole-mount in situ hybridization. *A–D*: Co-localization of PDX1 and *Ngn3*. *A*: *Ngn3* in situ hybridization signal viewed in normal light. *B*: PDX1 protein visualized by an immunofluorescent staining (green). *C*: False color image of *A*. *D*: Panels *B* and *C* merged. PDX1$^+$ cells are subdivided into *Ngn3*$^+$ (arrowheads) and *Ngn3*$^-$ (arrows) domains. *E–H*: *Ngn3* and PAX6 are expressed in distinct sets of cells. *E*: *Ngn3* in situ hybridization signal viewed in normal light. *F*: PAX6 protein visualized by an immunofluorescent staining (green). *G*: False color image of *E*. *H*: Panels *F* and *G* merged. PAX6$^+$ cells are separate from the *Ngn3*$^+$ cells (arrows), but are often found adjacent to *Ngn3*$^+$ cells (arrowheads). *I–L*: Expression of *Ngn3* and glucagon. *I*: *Ngn3* in situ hybridization signal viewed in normal light. *J*: Glucagon visualized by immunofluorescent staining (green). *K*: False color image of *I*. *L*: Panels *J* and *K* merged. GLU$^+$ cells (arrowheads) are separate from the *Ngn3*$^+$ cells (arrows).

The proliferating cell marker Ki-67 is expressed in *Ngn3*$^+$ but not in *NeuroD*$^+$ cells. If the *Ngn3*$^+$ cells represent a true endocrine precursor or stem cell population, we would expect these cells to divide. To examine whether *Ngn3*$^+$ cells were proliferating, we stained sections of *Ngn3* whole-mount in situ hybridizations for Ki-67, a marker of proliferating cells (32). Ki-67$^+$ nuclei are present within the *Ngn3*$^+$ domain (Fig. 6*A–D*), but absent from the *NeuroD*$^+$ domain (Fig. 6*E–H*). The lack of BrdU incorporation in E14 ISL1$^+$ cells corroborates the postmitotic nature of the endocrine cells at this stage (Fig. 6*I–K*). In contrast, endocrine cells are proliferating at E19, as visualized by BrdU incorporation in ISL$^+$ cells (Fig. 6*L–N*). Consistent with previous studies (33), we found that both α- and β-cells were proliferating at E19, as seen by BrdU incorporation into GLU$^+$ (Fig. 6*O–Q*) and Nkx6.1$^+$ cells (Fig. 6*R–T*).

Independent formation of α- and β-cells from epithelial precursor cells at the secondary transition. The issue of the origin of the pancreatic β-cells remains controversial. It has been proposed that β-cells originate from early PDX1$^+$/GLU$^+$ precursors through transient multihormonal cell types (5). Our proposal that postmitotic endocrine cells develop directly from proliferating *Ngn3*$^+$/GLU$^-$ precursor cells contradicts the lineage relationship proposed by Guz et al. (5) but is consistent with the proposal by Pang et al. (14), who showed that β-cells derive directly from the GLUT2$^+$ epithe-

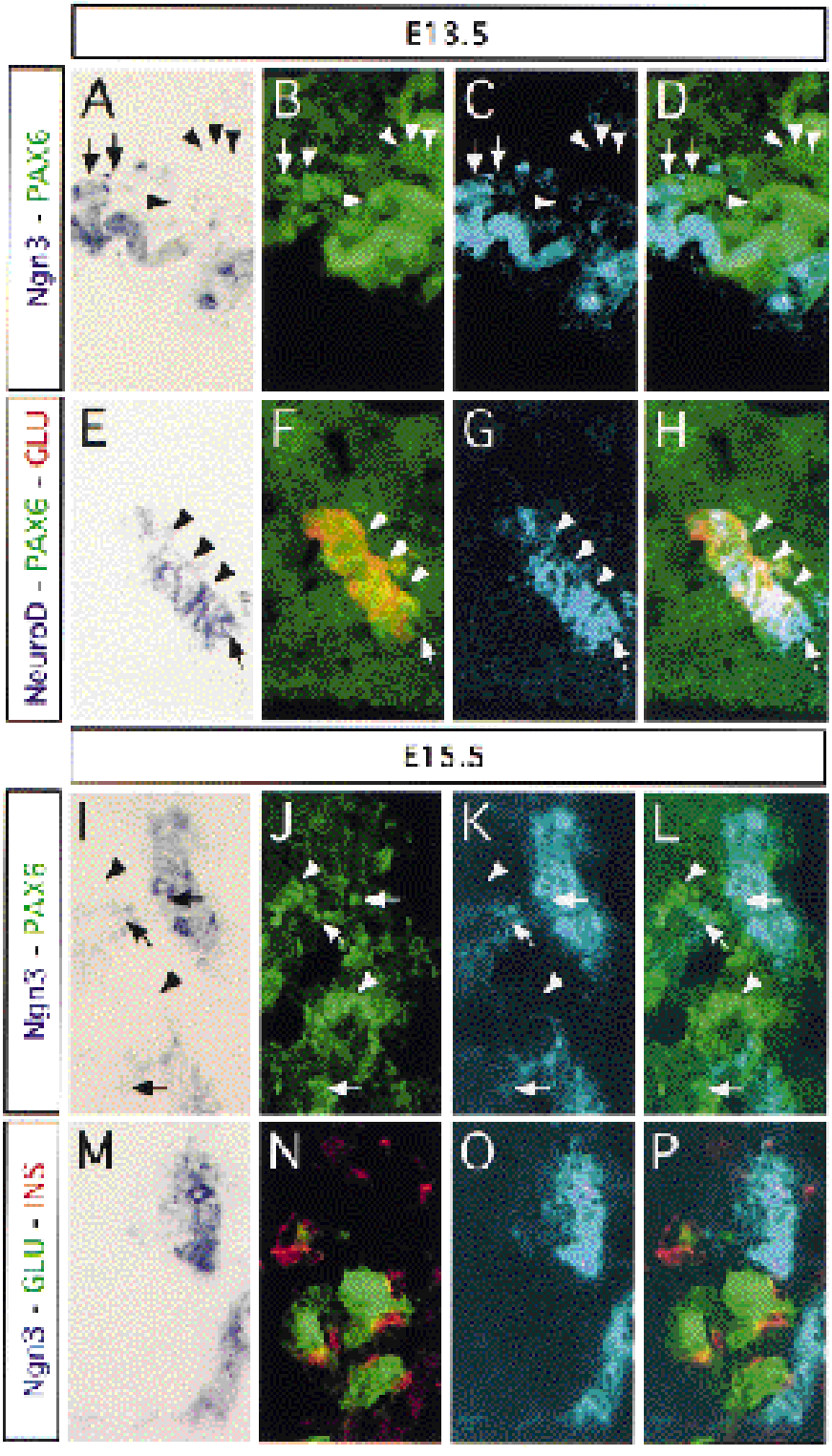

FIG. 4. *Neurogenin3* and *NeuroD* expression in E13.5 and E15.5 pancreas as detected in sections after whole-mount in situ hybridization. *A–D*: Expression of PAX6 and *Ngn3* at E13.5. *A*: *Ngn3* in situ hybridization signal viewed in normal light. *B*: PAX6 protein visualized by an immunofluorescent staining (green). *C*: False color image of *A*. *D*: Panels *B* and *C* merged. Most PAX6$^+$ cells are found outside the *Ngn3*$^+$ domain (arrowheads), but some PAX6$^+$ cells are within the *Ngn3*$^+$ domain (arrows). *E–H*: Co-localization of *NeuroD*, PAX6, and glucagon at E13.5. *E*: *NeuroD* in situ hybridization signal viewed in normal light. *F*: PAX6 (green) and glucagon (red) visualized by double immunofluorescent staining. *G*: False color image of *E*. *H*: Panels *F* and *G* merged. PAX6$^+$/GLU$^+$ cells are found in the *NeuroD*$^+$ domain (arrowheads), but *NeuroD*$^+$/PAX6$^-$/GLU$^-$ cells are also detectable (arrow). *I–L*: Expression of PAX6 and *Ngn3* at E15.5. *I*: *Ngn3* in situ hybridization signal viewed in normal light. *J*: PAX6 protein visualized by an immunofluorescent staining (green). *K*: False color image of *I*. *L*: Panels *J* and *K* merged. Most PAX6$^+$ cells are found outside the *Ngn3*$^+$ domain (arrowheads), but some PAX6$^+$ cells are within the *Ngn3*$^+$ domain (arrows). *M–P*: Expression of glucagon, insulin, and *Ngn3* at E15.5. *M*: *Ngn3* in situ hybridization signal viewed in normal light. *N*: Glucagon (green) and insulin (red) visualized by double immunofluorescent staining. *O*: False color image of *M*. *P*: Panels *N* and *O* merged. *Ngn3*$^+$ cells are distinct from GLU$^+$ and INS$^+$ cells.

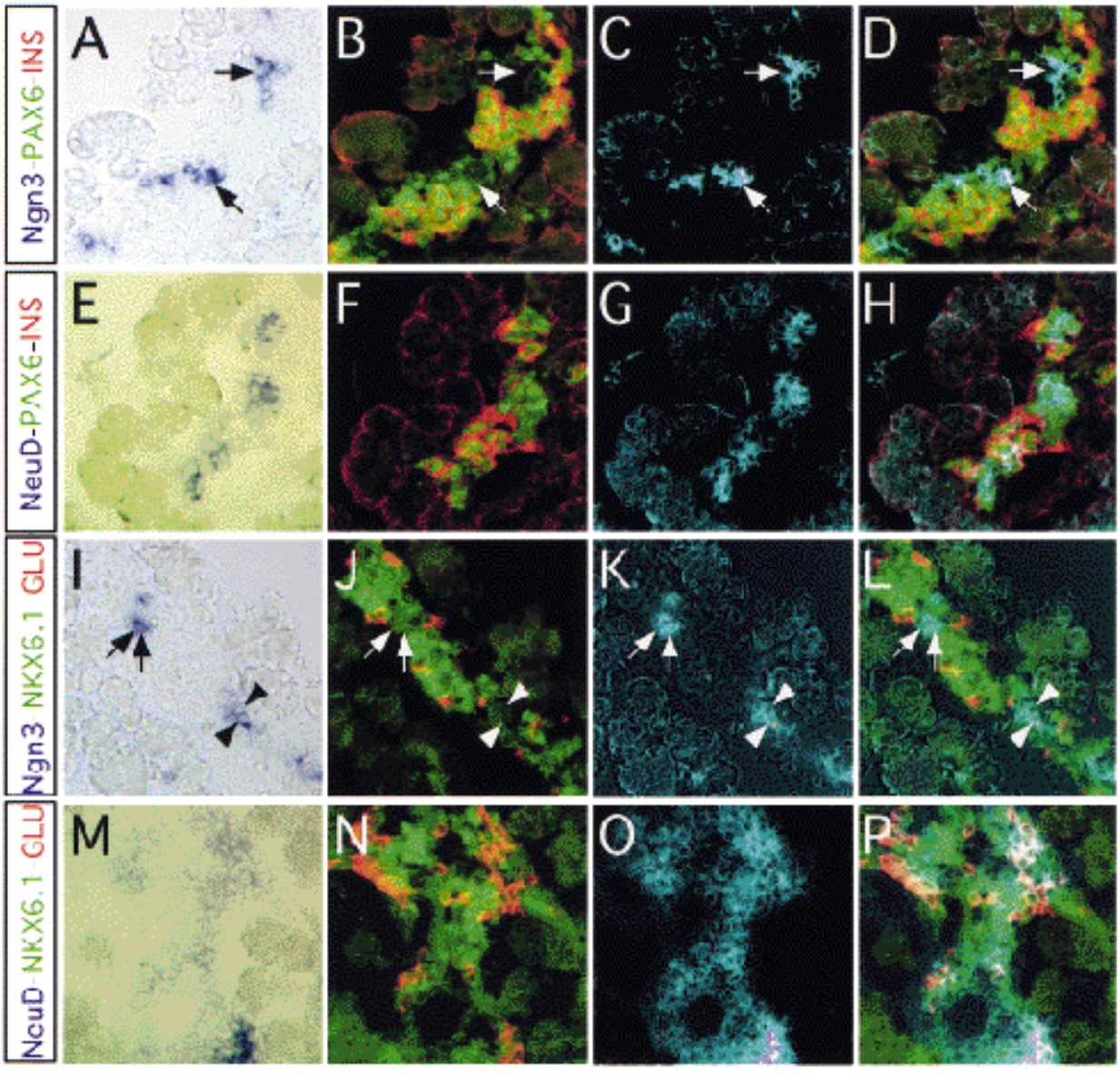

FIG. 5. *Neurogenin3* and *NeuroD* expression in E17.5 pancreas as detected in sections after whole-mount in situ hybridization. *A–D*: Expression of PAX6, insulin, and *Ngn3*. *A*: *Ngn3* in situ hybridization signal viewed in normal light. *B*: PAX6 (green) and insulin (red) visualized by double immunofluorescent staining. *C*: False color image of *A*. *D*: Panels *B* and *C* merged. PAX6$^+$ and INS$^+$ cells are found outside the *Ngn3*$^+$ domain (arrows). *E–H*: Co-localization of *NeuroD*, PAX6, and insulin. *E*: *NeuroD* in situ hybridization signal viewed in normal light. *F*: PAX6 (green) and insulin (red) visualized by double immunofluorescent staining. *G*: False color image of *E*. *H*: Panels *F* and *G* merged. PAX6$^+$/INS$^+$ cells are found in the *NeuroD*$^+$ domain. *I–L*: Expression of *Ngn3*, Nkx6.1, and glucagon. *I*: *Ngn3* in situ hybridization signal viewed in normal light. *J*: Nkx6.1 (green) and glucagon (red) visualized by double immunofluorescent staining. *K*: False color image of *I*. *L*: Panels *J* and *K* merged. Most Nkx6.1$^+$ cells are found outside the *Ngn3*$^+$ domain (arrowheads), but some Nkx6.1$^+$ cells are within the *Ngn3*$^+$ domain (arrows). GLU$^+$ cells are distinct from both Nkx6.1$^+$ and *Ngn3*$^+$ cells. *M–P*: Expression of *NeuroD*, Nkx6.1, and glucagon. *M*: *NeuroD* in situ hybridization signal viewed in normal light. *N*: Nkx6.1 (green) and glucagon (red) visualized by double immunofluorescent staining. *O*: False color image of *M*. *P*: Panels *N* and *O* merged. Nkx6.1^{high} and GLU$^+$ cells are found in separate sets of cells within the *NeuroD*$^+$ domain.

lium beginning at E13.5. However, the data shown above do not allow us to determine whether β-cells go through a transient GLU$^+$/PDX1$^+$ stage (5). We therefore decided to analyze the development of endocrine cells at the secondary transition by determining the expression pattern of *1*) transcription factors that precede the expression of hormones and are common to all endocrine cells and *2*) transcription factors specific to α- or β-cells.

We first studied ISL1 and PAX6 expression at E14. We found that all PAX6$^+$ cells co-expressed ISL1 (Fig. 7*A–C*), which was similar to the situation we found at E10. However, the presence of ISL1$^+$/PAX6$^-$cells were evident also at this stage (Fig. 7*A–C*), suggesting that endocrine cell development from hormone negative cells occurs at this stage. In an attempt to discriminate between α- and β-cells, we analyzed the expression of the α-cell marker BRN4 (34) in relation to ISL1, glucagon, and insulin. As shown in Fig. 7*D–F*, ISL1$^+$ cells can be divided into a BRN4$^+$ and a BRN4$^-$ population. Because we found expression of BRN4 in all glucagon-producing cells (Fig. 7*G–I*), we believe that the presence of BRN4$^+$/ISL1$^-$ cells is best explained by activation of BRN4 expression before ISL1$^-$ and, subsequently, glucagon expression in α-cell development. If this hypothesis is indeed

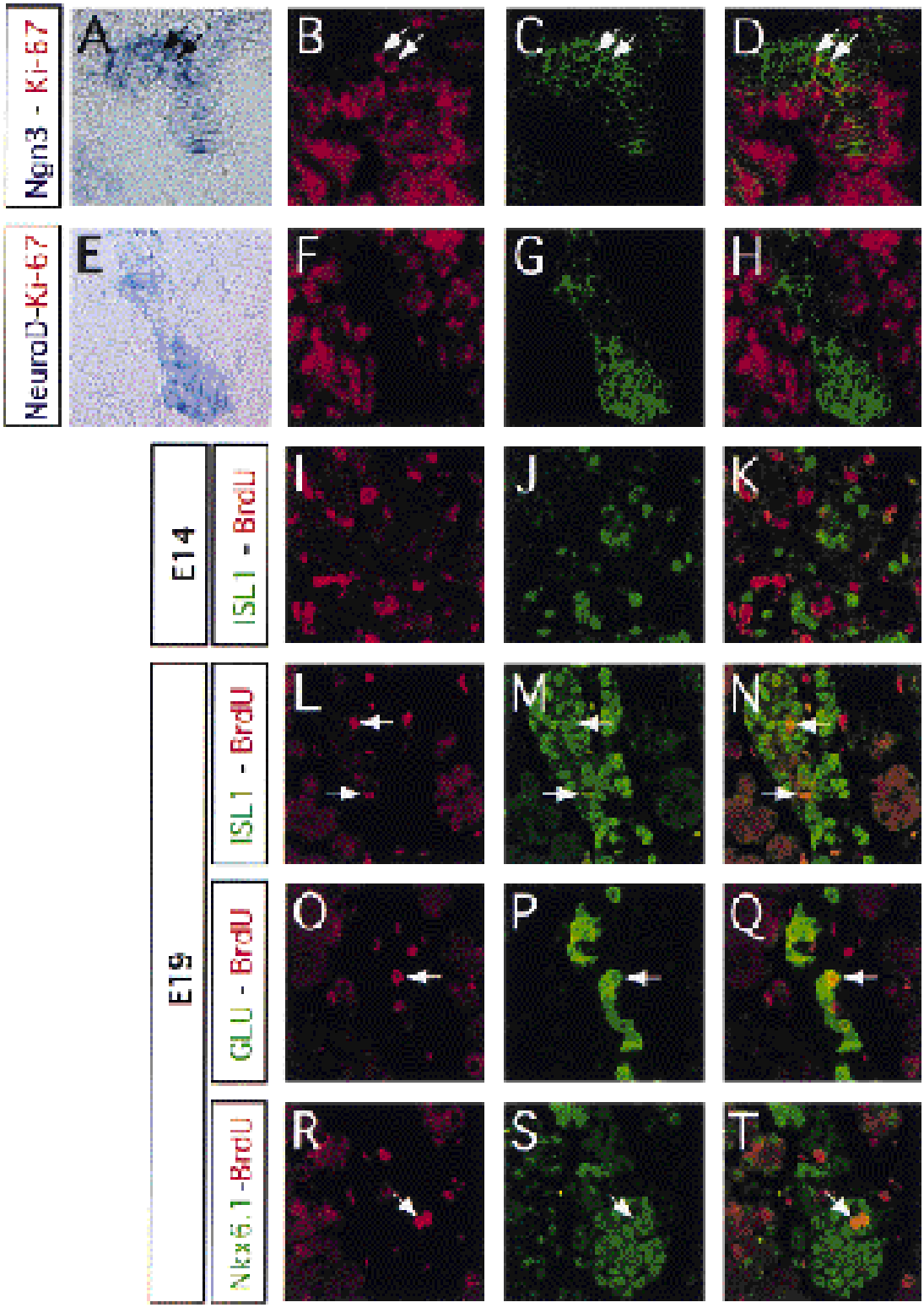

FIG. 6. $Ngn3^+$ cells are proliferating, whereas early endocrine cells are postmitotic. *A–D*: Co-expression of *Ngn3* and Ki-67 at E15.5. *A*: *Ngn3* in situ hybridization signal viewed in normal light. *B*: Ki-67 visualized by immunofluorescent staining (red). *C*: False color image of *A*. *D*: Panels *B* and *C* merged. Ki-67$^+$ cells are found within the $Ngn3^+$ domain (arrows). *E–H*: *NeuroD* and Ki-67 are expressed in distinct sets of cells at E13.5. *E*: *NeuroD* in situ hybridization signal viewed in normal light. *F*: Ki-67 visualized by immunofluorescent staining (red). *G*: False color image of *E*. *H*: Panels *F* and *G* merged. Ki-67$^+$ cells are found outside the $NeuroD^+$ domain. *I–T*: BrdU incorporation in E14 (*I–K*) and E19 (*L–T*) mouse pancreas. *I*, *L*, *O*, and *R*: BrdU visualized by immunofluorescent staining (red). *J*: ISL1 visualized by immunofluorescent staining (green). *K*: Panels *J* and *K* merged. There is no overlap between ISL1 and BrdU. *M*: ISL1 visualized by immunofluorescent staining (green). *N*: Panels *L* and *M* merged. Note the occasional overlap (yellow) between ISL1 and BrdU (arrows). *P*: Glucagon visualized by immunofluorescent staining (green). *Q*: Panels *O* and *P* merged. Note the occasional overlap (yellow) between glucagon and BrdU (arrow). *S*: Nkx6.1 visualized by immunofluorescent staining (green). *T*: Panels *R* and *S* merged. Note the occasional overlap (yellow) between Nkx6.1 and BrdU (arrow).

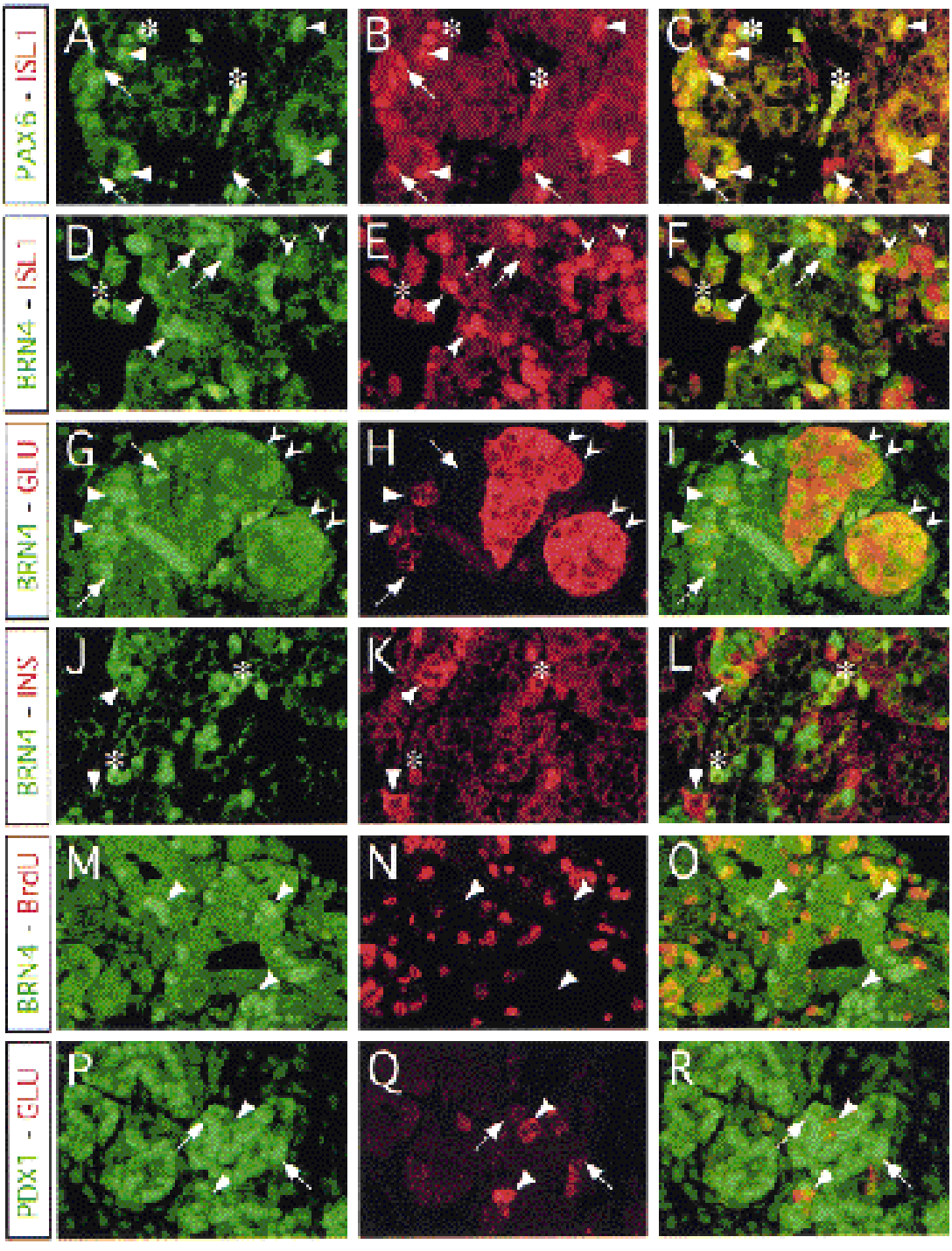

FIG. 7. BRN4 expression precedes ISL1 and glucagon expression during α-cell development in E14 mouse pancreas. *A–C*: ISL1 expression precedes PAX6 expression. *A*: PAX6 expression visualized by immunofluorescent staining (green). *B*: ISL1 expression visualized by immunofluorescent staining (red). *C*: Panels *A* and *B* merged. Note that all PAX6$^+$ cells are also ISL1$^+$ (yellow, arrowheads), whereas some ISL1$^+$ cells are PAX6$^-$ (arrows). *D–F*: BRN4 expression precedes ISL1 expression and defines two distinct ISL1$^+$ populations. *D*: BRN4 expression visualized by immunofluorescent staining (green). *E*: ISL1 expression visualized by immunofluorescent staining (red). *F*: Panels *D* and *E* merged. Note the presence of BRN4$^+$/ISL1$^+$ (yellow, arrowheads), BRN4$^+$/ISL1$^-$ (arrows), and BRN4$^-$/ISL1$^+$ cells (chevrons). *G–I*: BRN4 is an early marker of α-cells. *G*: BRN4 expression visualized by immunofluorescent staining (green). *H*: Glucagon expression visualized by immunofluorescent staining (red). *I*: Panels *G* and *H* merged. Note BRN4 expression in GLU$^-$ cells (arrows), newly formed GLU$^+$ cells (arrowheads), and mature GLU$^+$ cells (chevrons). *J–L*: β-Cells do not express BRN4 at E14. *J*: BRN4 expression visualized by immunofluorescent staining (green). *K*: Insulin expression visualized by immunofluorescent staining (red). *L*: Panels *J* and *K* merged. Note the absence of BRN4 expression in the INS$^+$ cells (arrowheads). *M–O*: BRN4$^+$ cells are postmitotic. *M*: BRN4 expression visualized by immunofluorescent staining (green). *N*: BrdU incorporation visualized by immunofluorescent staining (red). *O*: Panels *M* and *N* merged. Note the absence of BrdU incorporation in BRN4$^+$ cells (arrowheads). *P–R*: Scattered GLU$^+$ cells express low amounts of PDX1 at E14. *P*: PDX1 expression visualized by immunofluorescent staining (green). Note the presence of two populations of PDX1-expressing cells: low-level expression of PDX1$^+$ (arrowheads) and high-level expression of PDX1^{high} (arrows). *Q*: Glucagon expression visualized by immunofluorescent staining (red). *R*: Panels *P* and *Q* merged. Note that the GLU$^+$ cells are PDX1$^+$ (arrowheads), whereas PDX1^{high} cells do not produce glucagon (arrows). *Red blood cells.

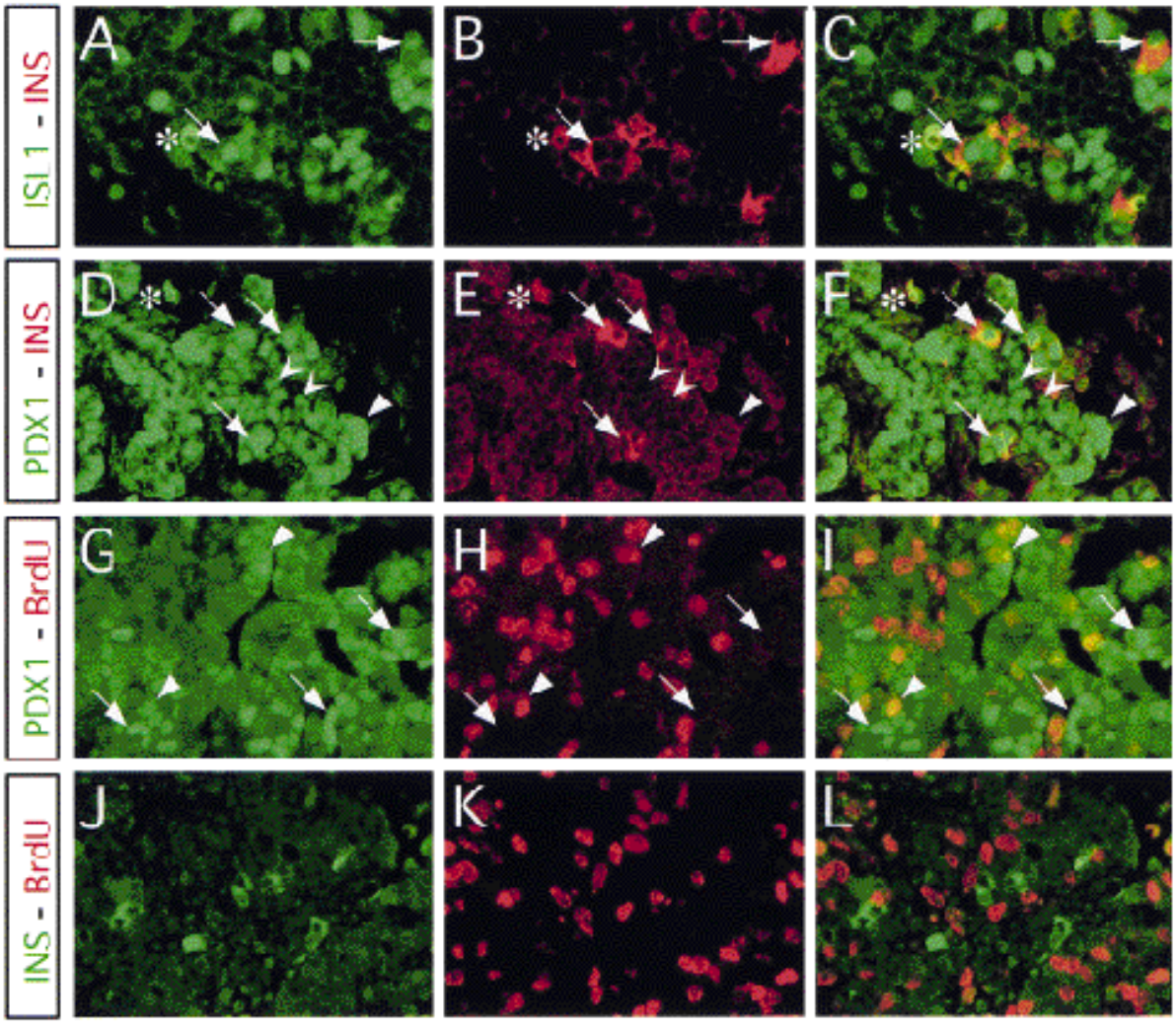

FIG. 8. β-Cells arise from postmitotic PDX1^{high} cells. *A–C*: INS$^+$ cells express ISL1. *A*: ISL1 expression visualized by immunofluorescent staining (green). *B*: Insulin expression visualized by immunofluorescent staining (red). *C*: Panels *A* and *B* merged. Note that INS$^+$ cells are also ISL1$^+$ (arrows). *D–F*: High-level PDX1 expression precedes insulin expression. *D*: PDX1 expression visualized by immunofluorescent staining (green). Note the presence of two populations of PDX1 expressing cells: low-level expression of PDX1$^+$ (chevrons) and high-level expression of PDX1^{high} (arrows and arrowheads). *E*: Insulin expression visualized by immunofluorescent staining (red). *F*: Panels *D* and *E* merged. Note the presence of INS$^+$/PDX1^{high} cells (arrows) and INS$^-$/PDX1^{high} cells (arrowheads). Low-level PDX1$^+$ cells are INS$^-$ (chevrons). *G–I*: PDX1^{high} cells are postmitotic. *G*: PDX1 expression visualized by immunofluorescent staining (green). *H*: BrdU incorporation visualized by immunofluorescent staining (red). *I*: Panels *G* and *H* merged. Note that PDX1^{high} cells do not incorporate BrdU (arrows), whereas low-level PDX1$^+$ cells often incorporate BrdU (arrowheads). *J–L*: β-Cells are postmitotic at E14. *J*: Insulin expression visualized by immunofluorescent staining (green). *K*: BrdU incorporation visualized by immunofluorescent staining (red). *L*: Panels *J* and *K* merged. Note the absence of BrdU incorporation in INS$^+$ cells. *Red blood cells.

valid, we should have found some BRN4$^+$/GLU$^-$ cells at this stage. As seen in Fig. 7*G–I*, such cells are readily detectable. The BRN4$^-$/ISL1$^+$ population most likely represents β-cells that express ISL1 (Fig. 8*A–C*) but not BRN4 (Fig. 7*J–L*). BRN4$^+$ cells did not incorporate BrdU during a 90-min pulse (Fig. 7*M–O*), which indicates that they are postmitotic. Whereas most GLU$^+$ cells were PDX1$^-$ at E14 (data not shown), we did see scattered GLU$^+$ cells that were PDX1$^+$ (Fig. 7*P–R*). However, cells that expressed high levels of PDX1 (PDX1^{high}) were not found to co-express glucagon at any stage (Fig. 7*P–R*).

As we have previously found in the rat (13), PDX1^{high} cells were often found to be INS$^+$ at E14 (Fig. 8*D–F*). However, PDX1^{high}/INS$^-$ cells were also found at E14 (Fig. 8*D–F*), suggesting that upregulation of PDX1 precedes INS production. The PDX1^{high} cells did not incorporate BrdU, whereas intermediate-level PDX1$^+$ cells did incorporate BrdU (Fig. 8*G–I*). Consistent with the absence of BrdU in PDX1^{high} cells and with the INS$^+$/PDX1^{high} co-expression, INS$^+$ cells were never found to incorporate BrdU at E14 (Fig. 8*J–L*).

Dynamic expression of Notch-1 and -2 during pancreas development. Mammalian homologs of the *Drosophila* hairy- and enhancer-of-split factors (HES proteins) are negatively acting bHLH proteins that antagonize members of the Ngn and NeuroD family (L. Flores, unpublished observations; 35,36). *Hes1* was the only member of the HES family that we detected in an RT-PCR screening for expression of these factors in the embryonic pancreas (data not shown). *Hes1* mutant animals display pancreatic hypoplasia due to accelerated differentiation of endocrine cells that results in a depletion of epithelial precursors (34a). As *Hes1* is a known downstream

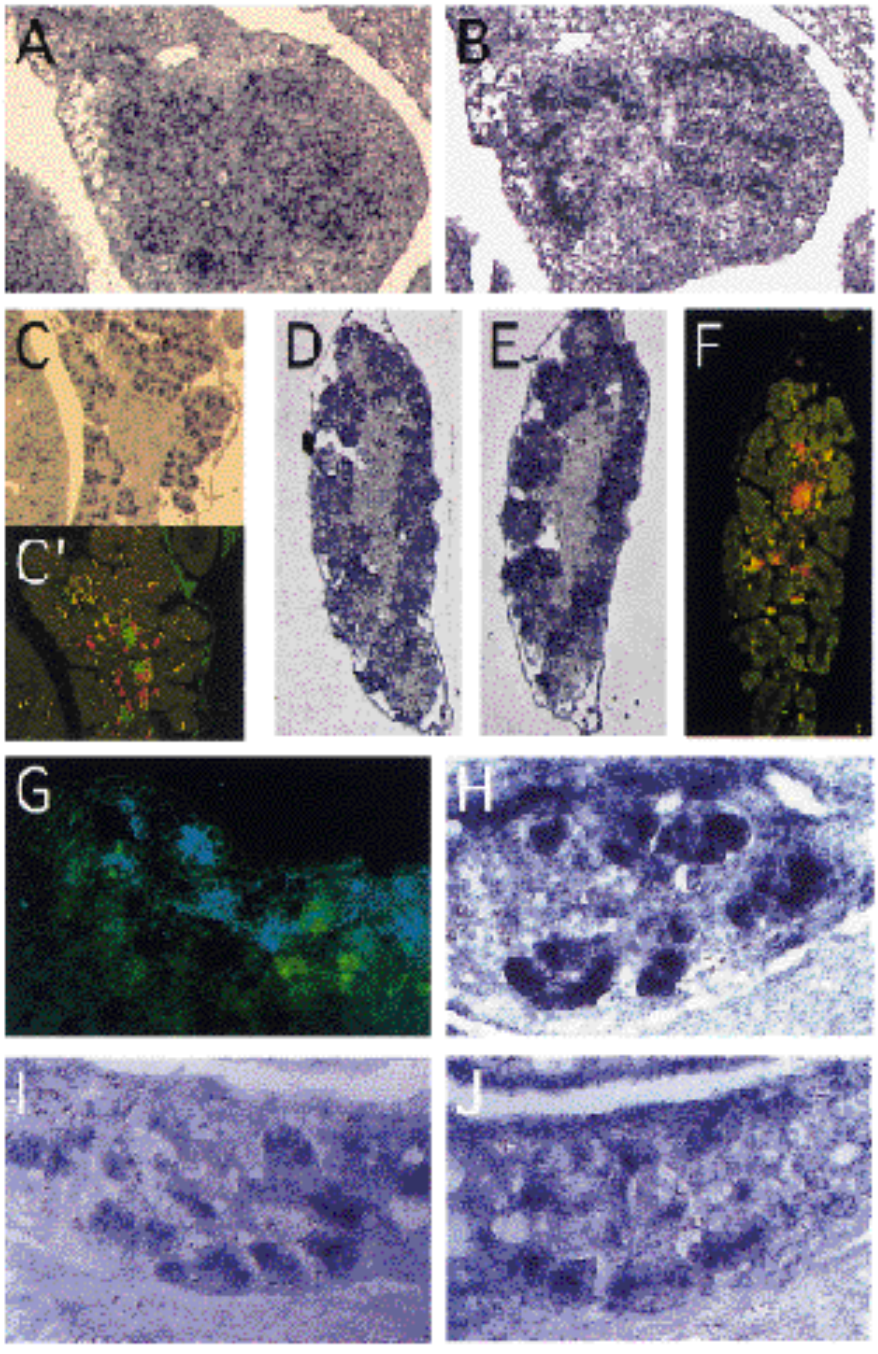

FIG. 9. Notch pathway components are expressed in the developing pancreas. *A* and *C–D*: *Notch-1* expression in E12 (*A*), E15 (*C* and *C′*), and E17 (*D*) mouse pancreas. High expression of *Notch-1* mRNA is seen in the epithelial cells at E12 and in forming acini at E15 and E17. *B*: *Notch-2* expression in E12 mouse pancreas. *C′*: Insulin (red) and glucagon (green) double immunofluorescent staining of a section adjacent to *C*. Note that the endocrine cells do not express *Notch-1*. *E*: *Notch-2* expression in mouse E17 acinar cells. *F*: Insulin (red) and glucagon (green) double immunofluorescent staining of a section adjacent to *E*. Note that the endocrine cells do not express *Notch-1* and *-2*. *G*: PAX6 and *Notch-1* expression in E13.5 mouse pancreas as detected in sections after whole-mount in situ hybridization. *Notch-1* in situ hybridization signal shown in false color (blue) and PAX6 immunofluorescent staining (green). Note that PAX6$^+$ cells are mainly located outside the *Notch-1*$^+$ domain, but some PAX6$^+$ cells are found inside the *Notch-1*$^+$ domain. *H–J*: Expression of *Jagged-1* (*H*), *Notch-1* (*I*), and *Notch-2* (*J*) in E13.5 rat pancreas epithelium.

component in the Notch-signaling system (37), we sought to identify if any of the mammalian Notch-factors were expressed during pancreatic development. We found that three mammalian *Notch* genes, *Notch-1*, *-2*, and *-3*, but not *Notch-4*, were expressed during pancreatic development (Fig. 10). In situ hybridization on sections of embryonic pancreas revealed that *Notch-1* is expressed in the epithelium at E12 (Fig. 9*A*). At E15.5, *Notch-1* mRNA is located in the forming exocrine tissue (Fig. 9*B*, *C*, and *C′*). At E17.5, localization of both *Notch-1* and *-2* in exocrine tissue and absence from endocrine tissue is evident (Fig. 9*D–F*). *Notch-1* is also absent from most endocrine cells at E13.5, although a few PAX6$^+$ cells are located still in the *Notch-1*$^+$ domain (Fig. 9*G*). Similar to the mouse, E13 rat pancreas expresses *Notch-1* and *-2* and

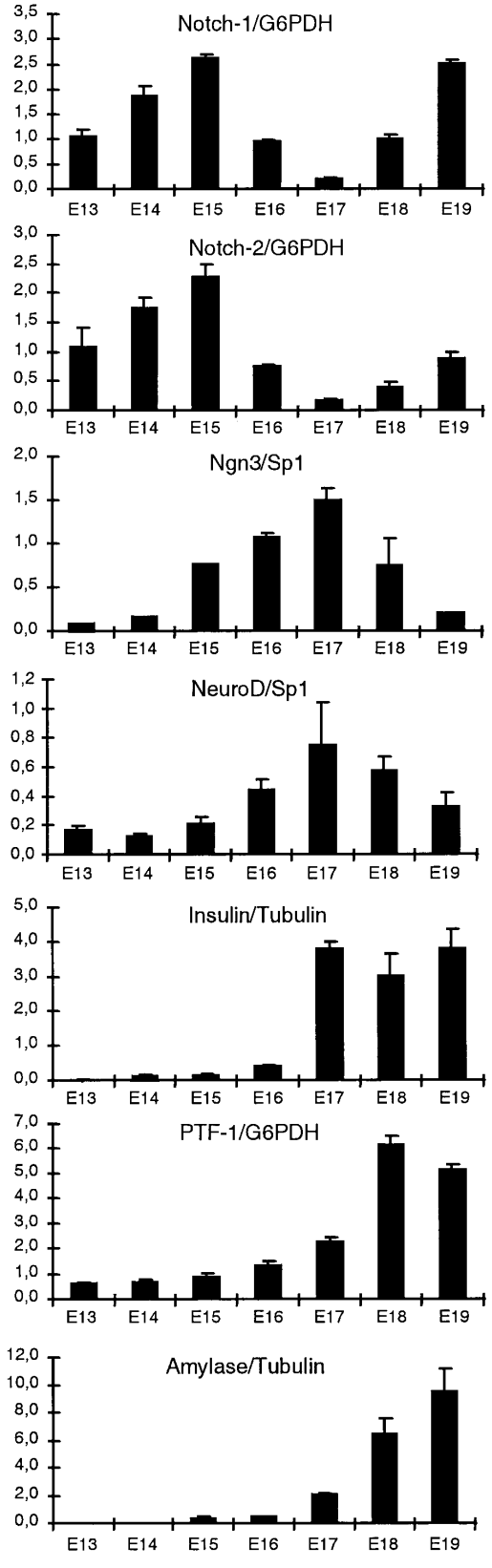

FIG. 10. Semiquantitative RT-PCR analysis of the expression of *Notch-1* and *-2*, *Ngn3*, *NeuroD*, *insulin*, *p48-PTF1*, and *amylase* in embryonic rat pancreas of the indicated stages of embryonic development. The ratio between the analyzed genes and the internal standard are shown. Note the decline in *Notch-1* and *-2* expression before or concomitant with the secondary transition that begins at E15–E15.5 in the rat.

Jagged1 primarily in the epithelial cells and significantly in the mesenchyme (Fig. 9*H–J*). RT-PCR analysis of microdissected rat embryonic pancreas revealed that *Notch-1*, *-2*, and *-3* are expressed at increasing levels until E15.5 and followed by a marked decline in the next 2 days (Fig. 10). A second phase of high expression occurs after the secondary transition (Fig. 10). The decline in Notch gene expression appears at the onset of the secondary transition and is marked by increased expression of insulin and amylase (Fig. 10). Furthermore, the increase in *NeuroD* and *p48-PTF1* gene expression is similarly observed between E16.5 and E17.5 (Fig. 10). In light of the reported expression of the Notch ligands *Dll1* in a few pancreatic epithelial cells and *Jagged1* in most pancreatic epithelial cells (38,39), the *Notch-1* expression pattern at this stage suggests that Notch-1 is transducing a signal that counteracts endocrine differentiation.

DISCUSSION

In this study, we have shown that the early proliferating epithelium of the pancreas, which uniformly expressed the homeodomain protein PDX1, can be subdivided into *Ngn3*$^+$ and *Ngn3*$^-$ subpopulations. We speculate that the *Ngn3*$^-$ population represents exocrine precursor cells that express *p48-PTF1*. By conducting an extensive marker analysis, combined with an evaluation of the proliferative status of cell types defined by the markers, we purport that there is a temporal sequence of gene (in)activation for developing α- and β-cells. Moreover, we propose that endocrine cells develop directly from a dividing *Ngn3*$^+$/PDX1$^+$/Nkx6.1$^+$/Ki-67$^+$ population into a nondividing *NeuroD*$^+$/ISL1$^+$/PAX6$^+$/Ki-67$^-$ cell throughout the process of pancreas development (Fig.11*A*). Intermediate stages in this process are marked by the sequential appearance of specific transcription factors. For developing α-cells, this sequence appears to occur in the following order: *NeuroD*^{on} – *Brn4*^{on} – *Isl1*^{on} – *Pax6*^{on} – *Ngn3*^{off} – *GLU*^{on} – *Pdx1*^{off}/*nkx6.1*^{off} (Fig. 11*B*). A similar sequence for developing β-cells is proposed: *NeuroD*^{on} – *Isl1*^{on} – *Pax6*^{on} – *Ngn3*^{off} – *Pdx1*^{high}/*nkx6.1*^{high} – *INS*^{on} (Fig. 11*B*), while *Pax4* is likely to play an instructive role (40) at an early but as yet undetermined stage. In both cases, cell cycle exit would occur before NeuroD gene activation. Our data strongly support the alternative developmental pathway for endocrine cells proposed by Pang et al. (14) and Herrera et al. (9); our model can be considered an extension of their models. We do not believe that PDX1$^+$/GLU$^+$ cells can be precursors for β-cells (5). We base this conclusion on the following observations: *1*) we and others (10) did not observe BrdU incorporation in GLU$^+$ cells until stages well after the formation of β-cells and before E19, well after the β-cells had formed; *2*) GLU-promoter-toxigene transgenic mice had normal β-cell formation (9); *3*) there was a lack of BRN4 expression in INS$^+$ cells; and *4*) the number of PDX1$^+$/GLU$^+$ cells is insufficient to account for the large increase in β-cell mass seen at the secondary transition. Our conclusions do not challenge the presence of INS$^+$/GLU$^+$ cells, but we believe that such cells do not exist as precursors for mature β-cells. Like other studies, we found INS$^+$/GLU$^+$ cells before but not after E14. However, these cells are scarce and express insulin at low levels, and they are always associated with GLU$^+$ cell clusters. In the rat, such cells, unlike mature β-cells (13), do not express high levels of PDX1 and Nkx6.1. These findings indicate that INS$^+$/GLU$^+$ cells represent a

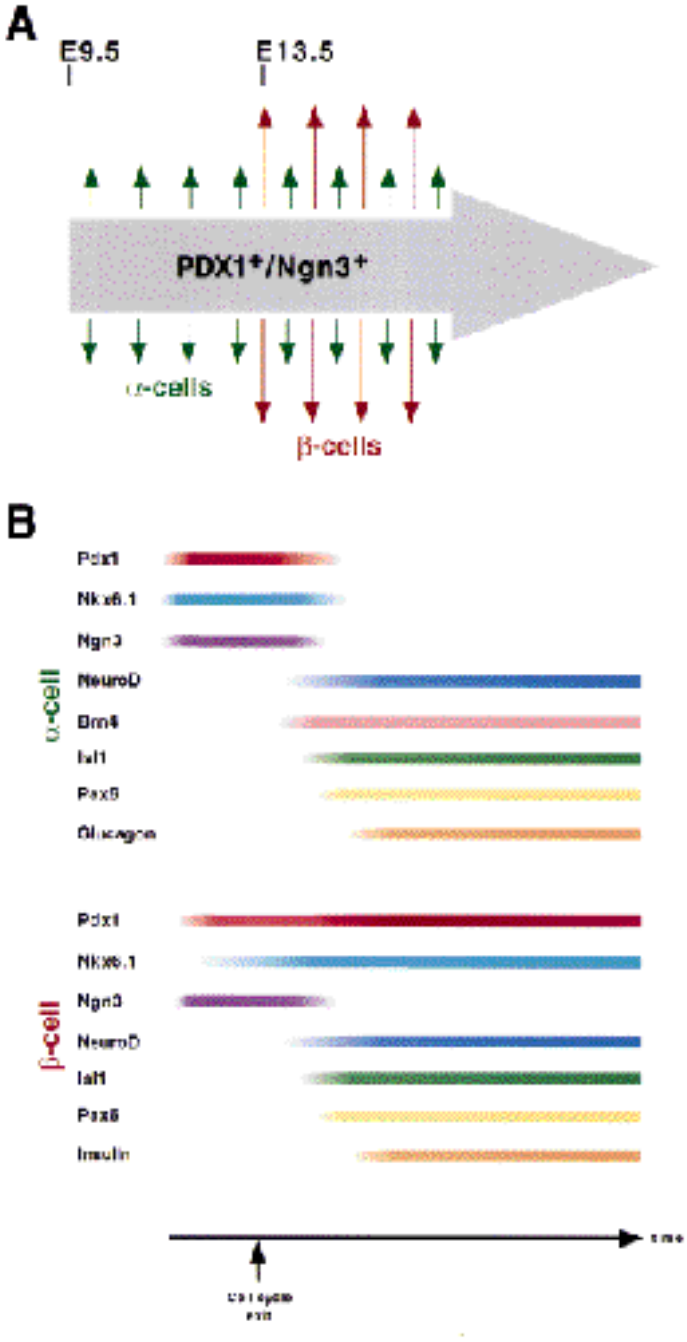

FIG. 11. Model of mouse endocrine pancreas differentiation. *A*: α-Cells are formed from proliferating PDX1$^+$/Ngn3$^+$ epithelial cells throughout pancreas ontogeny, whereas formation of β-cells only begins in significant numbers at E13.5. *B*: Proposed temporal sequence of gene (in)activation during α- and β-cell differentiation based on the marker analysis of this study.

fraction of α-cells that are capable of expressing insulin transiently, as suggested by Larsson (41).

The requirement for *Ngn1* and/or *Ngn2* for *NeuroD* gene activation in certain neuronal cells (17,18) suggests that *Ngn3* might play a similar role in the pancreas. Indeed, *Ngn3* mutant mice fail to activate *NeuroD* expression and lack all endocrine cells (F. Guillemot, G. Gradwohl, personal communication), and expression of *Ngn3* in transgenic mice under control of the *Pdx1* promoter results in excessive endocrine differentiation at the expense of exocrine differentiation (42). The importance of *Ngn3* for *NeuroD* activation and endocrine differentiation raises an important question: what prevents the *Ngn3*$^+$/Ki-67$^+$ cells from leaving the cell cycle, activating *NeuroD*, and differentiating? The presence of Notch-1 and -2 (this study and 42), and the Notch ligands Jagged1 (also known as Serrate1) and Dll1 (this study and 38,39,42) in the pancreatic epithelium suggests that the Notch pathway could provide a inhibitory signal and thereby prevent premature differentiation of *Ngn3*$^+$ precursor cells. Indeed, mice deficient for *RBP-J* κ and *HES-1*, two components in the pathway downstream of Notch, show precocious differentiation of endocrine cells (34a,42). Furthermore, mice that have Notch-1 activity inhibited in the pancreatic epithelium by targeted misexpression of a constitutively active form of Notch-3 under control of the *Pdx1* promoter display a similar phenotype (42). The role of the Notch ligands is likely to be more complicated. Mice deficient for *Dll1* also show premature differentiation (42). However, the cellular distribution of *Dll1* transcripts in the pancreatic epithelium is unknown, which makes it difficult to make a precise model. Assuming that *Dll1* is expressed in endocrine cells, we envisioned a model in which the differentiated endocrine cells inhibit further differentiation of neighboring epithelial cells (lateral inhibition). However, the expression of several ligands with distinct temporal profiles suggests that a lateral inhibition model might be only part of the picture. Additionally, Notch signaling might also be required for repression of *Ngn3* expression in the *Ngn3*$^-$/PDX1$^+$ epithelial cells and maintenance of *p48-PTF1* expression in these cells (42), which would allow proper expansion of exocrine precursors. To speculate that activation and/or maintenance of *Jagged* and *Notch* expression in the epithelium requires a signal from the mesenchyme is tempting. Throughout pancreatic development, the mesenchymal-to-epithelial mass ratio continuously declines, and the rapid decline of *Notch* expression immediately before the secondary transition could be caused by the relative reduction of such a mesenchymal signal. This notion is consistent with the outcome of experiments in which pancreatic epithelium is cultured separately from the mesenchyme. Epithelium cultured alone does not proliferate; if cultured in supportive matrix or under the kidney capsule, endocrine differentiation proceeds by default (43–45). Hypothetically, this result is expected if *Jagged* or *Notch* expression depends on a mesenchymal signal and if Notch signaling is needed to maintain the undifferentiated state and *p48-PTF1* expression. We are currently investigating the effects on *Notch* and *Jagged* expression after removal of the mesenchyme. In conclusion, we present a marker analysis of developing α- and β-cells that strongly suggests that these two cell types are derived independently of each other from a *Ngn3*-expressing subset of the PDX1$^+$ pancreatic epithelial cells, and that proper timing of differentiation relies on inhibitory signals from the Notch pathway. An understanding of this pathway may lead to controlled expansion and differentiation of β-cell precursors in vitro and, thus, may provide an unlimited source of β-cells for transplantation.

ACKNOWLEDGMENTS

This work was supported by a grant from the National Institutes of Health (DK-55284), by the Juvenile Diabetes Foundation International, and by the Danish National Research Foundation.

We are grateful to F. Guillemot for sharing research data before publication and for providing the Ngn3 cDNA. We thank J. Hald and F.G. Andersen for providing Notch-1 and -2 and NeuroD probes, respectively, and S. Saule and M. Rosenfeld for providing PAX6 and BRN4 antibodies.

REFERENCES

1. Han J, Rall L, Rutter W: Selective expression of rat pancreatic genes during embryonic development. *Proc Natl Acad Sci U S A* 83:110–114, 1986
2. Pictet R, Rutter W: Development of the embryonic pancreas. In *Handbook of Physiology*. Sec. 1, vol. 1. Steiner D, Freinkel N, Eds. Washington, DC, American Physiologic Society, 1972, p. 67–76
3. Wessels N, Cohen J: Early pancreas organogenesis: morphogenesis, tissue interactions, and mass effects. *Dev Biol* 15:237–270, 1967
4. Pictet R, Clark W, Williams R, Rutter W: An ultrastructural analysis of the developing embryonic pancreas. *Dev Biol* 29:436–467, 1972
5. Guz Y, Montminy M, Stein R, Leonard J, Gamer L, Wright C, Teitelman G: Expression of murine STF-1, a putative insulin gene transcription factor, in beta cells of pancreas, duodenal epithelium and pancreatic exocrine and endocrine progenitors during ontogeny. *Development* 121:11–18, 1995
6. Alpert S, Hanahan D, Teitelman G: Hybrid insulin genes reveal a developmental lineage for pancreatic endocrine cells and imply a relationship with neurons. *Cell* 53:295–308, 1988
7. Madsen O, Serup P, Karlsen C, Lund K, Petersen H, Blume N, Andersen F, Jensen J, Michelsen B: A tumour model for the study of islet cell differentiation. *Biochem Soc Trans* 21:142–146, 1993
8. Madsen O, Larsson L, Rehfeld J, Schwartz T, Lernmark A, Labrecque A, Steiner D: Cloned cell lines from a transplantable islet cell tumor are heterogeneous and express cholecytokinin in addition to islet hormones. *J Cell Biol* 103:2025–2034, 1986
9. Herrera PL, Huarte J, Zufferey R, Nichols A, Mermillod B, Philippe J, Muniesa P, Sanvito F, Orci L, Vassalli JD: Ablation of islet endocrine cells by targeted expression of hormone-promoter-driven toxigenes. *Proc Natl Acad Sci U S A* 91:12999–13003, 1994
10. Ahlgren U, Pfaff S, Jessell T, Edlund T, Edlund H: Independent requirement for ISL1 in formation of pancreatic mesenchyme and islet cells. *Nature* 385: 257–260, 1997
11. Jonsson J, Carlsson L, Edlund T, Edlund H: Insulin-promoter-factor 1 is required for pancreas development in mice. *Nature* 371:606–609, 1994
12. Offield MF, Jetton TL, Labosky PA, Stein R, Magnuson MA, Hogan BLM, Wright CVE: Pdx-1 is required for pancreatic outgrowth and differentiation of the rostral duodenum. *Development* 122:983–995, 1996
13. Øster A, Jensen J, Serup P, Galante P, Madsen OD, Larsson LI: Rat endocrine pancreatic development in relation to two homeobox gene products (Pdx-1 and Nkx 6.1). *J Histochem Cytochem* 46:707–715, 1998
14. Pang K, Mukonoweshuro C, Wong GG: Beta cells arise from glucose transporter type 2 (Glut2)-expressing epithelial cells of the developing rat pancreas. *Proc Natl Acad Sci U S A* 91:9559–9563, 1994
15. Scharfmann R, Tazi A, Polak M, Kanaka C, Chernichow P: Expression of functional nerve growth factor receptors in pancreatic β-cell lines and fetal rat islets in primary culture. *Diabetes* 42:1829–1836, 1993
16. Edlund H: Transcribing pancreas. *Diabetes* 47:1817–1823, 1998
17. Ma Q, Chen Z, del Barco Barrantes I, de la Pompa JL, Anderson DJ: Neurogenin1 is essential for the determination of neuronal precursors for proximal cranial sensory ganglia. *Neuron* 20:469–482, 1998
18. Fode C, Gradwohl G, Morin X, Dierich A, LeMeur M, Goridis C, Guillemot F: The bHLH protein NEUROGENIN2 is a determination factor for epibranchial placode-derived sensory neurons. *Neuron* 20:483–494, 1998
19. Jensen J, Serup P, Karlsen C, Nielsen TF, Madsen OD: mRNA profiling of rat islet tumors reveals nkx 6.1 as a beta-cell-specific homeodomain transcription factor. *J Biol Chem* 271:18749–18758, 1996
20. Stoffers DA, Stanojevic V, Habener JF: Insulin promoter factor-1 gene mutation linked to early-onset type 2 diabetes mellitus directs expression of a dominant negative isoprotein. *J Clin Invest* 102:232–241, 1998
21. Turque N, Plaza S, Radvanyi F, Carriere C, Saule S: Pax-QNR/Pax-6, a paired box- and homeobox-containing gene expressed in neurons, is also expressed in pancreatic endocrine cells. *Mol Endocrinol* 8:929–938, 1994
22. Thor S, Ericson J, Brannstrom T, Edlund T: The homeodomain LIM protein Isl-1 is expressed in subsets of neurons and endocrine cells in the adult rat. *Neuron* 7:881–889, 1991
23. Blume N, Petersen JS, Andersen LC, Kofod H, Dyrberg T, Michelsen BK, Serup P, Madsen OD: Immature transformed rat islet beta-cells differentially express C-peptides derived from the genes coding for insulin I and II as well as a transfected human insulin gene. *Mol Endocrinol* 6:299–307, 1992
24. Hume C, Dodd J: Cwnt-8C: a novel Wnt gene with a potential role in primitive streak formation and hindbrain organization. *Development* 119:1147–1160, 1993
25. Borges M, Linnoila RI, van de Velde HJ, Chen H, Nelkin BD, Mabry M, Baylin SB, Ball DW: An achaete-schute homologue essential for neuroendocrine differentiation in the lung. *Nature* 386:852–855, 1997
26. Mutoh H, Fung BP, Naya FJ, Tsai MJ, Nishitani J, Leiter AB: The basic helix-loop-helix transcription factor BETA2/NeuroD is expressed in mammalian enteroendocrine cells and activates secretin gene expression. *Proc Natl Acad Sci U S A* 94:3560–3564, 1997
27. Mutoh H, Naya FJ, Tsai MJ, Leiter AB: The basic helix-loop-helix protein BETA2 interacts with p300 to coordinate differentiation of secretin-expressing enteroendocrine cells. *Genes Dev* 12:820–830, 1998
28. Naya F, Stellrecht C, Tsai M: Tissue-specific regulation of the insulin gene by a novel basic helix-loop-helix transcription factor. *Genes Dev* 9:1009–1019, 1995
29. Naya FJ, Huang HP, Qiu Y, Mutoh H, DeMayo FJ, Leiter AB, Tsai MJ: Diabetes, defective pancreatic morphogenesis, and abnormal enteroendocrine differentiation in BETA2/neuroD-deficient mice. *Genes Dev* 11:2323–2334, 1997
30. Chen H, Thiagalingam A, Chopra H, Borges MW, Feder JN, Nelkin BD, Baylin SB, Ball DW: Conservation of the Drosophila lateral inhibition pathway in human lung cancer: a hairy-related protein (HES-1) directly represses achaete-scute homolog-1 expression. *Proc Natl Acad Sci U S A* 94:5355–5360, 1997
31. Sommer L, Ma Q, Anderson DJ: Neurogenins, a novel family of atonal-related bHLH transcription factors, are putative mammalian neuronal determination genes that reveal progenitor cell heterogeneity in the developing CNS and PNS. *Mol Cell Neurosci* 8:221–241, 1996
32. Cattoretti G, Becker MH, Key G, Duchrow M, Schlüter C, Galle J, Gerdes J: Monoclonal antibodies against recombinant parts of the Ki-67 antigen (MIB 1 and MIB 3) detect proliferating cells in microwave-processed formalin-fixed paraffin sections. *J Pathol* 168:357–363, 1992
33. Hellerstrom C, Andersson A, Gunnarsson R: Regeneration of islet cells. *Acta Endocrinol Suppl (Copenh)* 205:145–160, 1976
34. Hussain M, Lee J, Miller C, Habener J: POU domain transcription factor Brain 4 confers pancreatic α-cell-specific expression of the proglucagon gene through interaction with a novel proximal promoter G1 element. *Mol Cell Biol* 17:7186–7194, 1997

34a. Jensen J, Pedersen EE, Galante P, Hald J, Heller RS, Ishibashi M, Kageyama R, Guillemot F, Serup P, Madsen OD: Control of endodermal endocrine development by Hes-1. *Nat Genet* 24:36–44, 2000

35. Ohtsuka T, Asahi M, Matsuura N, Kikuchi H, Hojo M, Kageyama R, Ohkubo H, Hoshimaru M: Regulated expression of neurogenic basic helix-loop-helix transcription factors during differentiation of the immortalized neuronal progenitor cell line HC2S2 into neurons. *Cell Tissue Res* 293:23–29, 1998
36. Kageyama R, Ishibashi M, Takebayashi K, Tomita K: bHLH transcription factors and mammalian neuronal differentiation. *Int J Biochem Cell Biol* 29: 1389–1399, 1997
37. Jarriault S, Brou C, Logeat F, Schroeter E, Kopan R, Israel A: Signalling downstream of activated mammalian Notch. *Nature* 377:355–358, 1995
38. Beckers J, Clark A, Wunsch K, Hrabe de Angelis M, Gossler A: Expression of the mouse Delta1 gene during organogenesis and fetal development. *Mech Dev* 1–2:165–168, 1999
39. Mitsiadis TA, Henrique D, Thesleff I, Lendahl U: Mouse Serrate-1 (Jagged-1): expression in the developing tooth is regulated by epithelial mesenchymal interactions and fibroblast growth factor-4. *Development* 124:1473–1483, 1997
40. Sosa-Pineda B, Chowdhury K, Torres M, Oliver G, Gruss P: The Pax4 gene is essential for differentiation of insulin-producing beta cells in the mammalian pancreas. *Nature* 386:399–402, 1997
41. Larsson L-I: On the development of the islet of Langerhans. *Microsc Res Tech* 43:284–291, 1998
42. Apelqvist Å, Li H, Sommer L, Beatus P, Anderson D, Honjo T, Hrabe de Angelis M, Lendahl U, Edlund H: Notch signalling controls pancreatic cell differentiation. *Nature* 400:877–881, 1999
43. Miralles F, Czernichow P, Scharfmann R: Follistatin regulates the relative proportions of endocrine versus exocrine tissue during pancreatic development. *Development* 125:1017–1024, 1998
44. Miralles F, Serup P, Cluzead F, Vandewalle A, Czerchinow P, Scharfmann R: Characterization of beta cells developed in vitro from rat embryonic pancreatic epithelium. *Dev Dyn* 214:116–126, 1999
45. Gittes G, Galante P, Hanahan D, Rutter W, Debase H: Lineage-specific morphogenesis in the developing pancreas: role of mesenchymal factors. *Development* 122:439–447, 1996